

# Real Flow Limitations in Supersonic Airplane Design

Robert M. Kulfan and Armand Sigalla  
*Boeing Commercial Airplane Company, Seattle, Wash.*

## I. Introduction

THE design of efficient supersonic airplanes with very highly swept wings is one of the more difficult problems in aeronautics. Highly swept wings are of interest because they have the potential, according to theory, of having relatively low drag at supersonic lifting conditions. Well-known supersonic wing theory<sup>1</sup> indicates that to achieve the low drag at lifting conditions, the leading edge of a wing must be at an angle of sweepback greater than the angle weak shockwaves make with the freestream at corresponding Mach numbers (subsonic leading edge). Sweepback angles of 70 to 75 deg are necessary for Mach numbers in the range of 2.0 to 3.0. Theoretical predictions indicate that an airplane with a wing of such high sweep would have an advantage of approximately 15 to 20% in lift/drag ratio when compared to an airplane having a much lower sweepback angle (for example, 50 deg).

When attempts were first made to substantiate these very encouraging predictions with wind-tunnel models, it was found that the experimental results did not confirm them at all. Subsequent examinations revealed that the low drag predicted by theory was not achieved because the flow pattern around the wings, implicit in theory, did not occur in practice. Viscosity, which normally has a relatively small effect on the overall flow over wings at normal cruise lift conditions, had a substantial effect on these highly swept wings.

Consider as an example a wing at Mach 3.0 and at an angle of attack of 4 deg—typical supersonic conditions. With the wing swept 75 deg to achieve low drag, the Mach number component normal to the leading edge is 0.78. Hence, near the wing leading edge, a recognized subsonic flow condition is

produced. The leading-edge flow is governed by the angle normal to the leading edge. Using simple sweep theory, the normal angle of attack for this example is found to be approximately 15 deg. Experience indicates that the airstream normally will not be able to flow around the leading edge at this large angle of attack without flow separation. This is particularly true for the thin airfoils that are characteristic of supersonic wing designs. This leading-edge flow separation completely alters the character of the flow pattern over the wing.

Leading-edge flow separation is only one of the reasons why the predicted low drag levels of highly swept wings could not be obtained. The trailing edge of these highly swept wings is generally at an angle of sweepback less than the weak shock wave angle (supersonic trailing edge). The flow over the wing, which is at a relatively low pressure, must therefore adjust to freestream pressure through a shock wave at the trailing edge. If the theoretical flow requires too large a pressure rise, significant trailing-edge separation occurs. Again, the flow pattern postulated by theory cannot occur, and the theoretical drags cannot be achieved. Similar problems can occur on other parts of such a highly swept wing. The establishment of a flow consistent with theoretical low drag is, therefore, contingent on the response of the boundary layer to potentially severe conditions all over the wing. The development and behavior of highly swept wing boundary layers under complicated three-dimensional flow conditions is not amenable to theoretical calculations.<sup>2</sup> Necessary wing design limitations cannot be defined strictly on the basis of analytical studies, and therefore have to be developed from experimental test programs.

---

Robert M. Kulfan joined the Boeing Company in 1960. During his first ten years with Boeing, as a member of the Supersonic Transport group, he participated in the development of aeronautical design and analysis methods, and was involved in extensive experimental and analytical SST configuration development studies. Since 1970 he has been the technical coordinator on a number of Boeing and government sponsored advanced technology system studies. He currently is a senior specialist engineer in Preliminary Design. He has authored and co-authored papers on subsonic aerodynamic technology applications, laminar flow control applications, hypersonic and supersonic aerodynamic interference, and leading edge vortex flow on highly swept wings. He received his BSE (1959) and MSE (1960) from the University of Michigan. He is a member of AIAA.

Armand Sigalla joined the Boeing Company in 1958 to do supersonic aerodynamic research relative to the Supersonic Transport program after four years of fluid mechanics research in England and Canada. In 1969, he was Flight Technology Manager for Boeing Phase B Space Shuttle proposal. Mr. Sigalla has been technology manager on the Boeing NASA Advanced Technology Transport Program. He currently is Chief of Technology—Preliminary Design, working on supersonic and subsonic transport airplanes. He is manager of the NASA Supersonic (SCAR) contracts for the Boeing Commercial Airplane Company. He has authored and co-authored papers on heat conduction, jet flow, boundary layer, sonic boom, nacelle/airframe interference, and advanced airplane design. He is an Associate Fellow of AIAA; Associate Fellow of the Royal Aeronautical Society, Associate City and Guilds Institute, London, and a member of the AIAA Committee on Aircraft Design.

---

Presented as Paper 78-147 at the AIAA 16th Aerospace Sciences Meeting, Huntsville, Ala., Jan. 16-18, 1978; received May 26, 1978; revision received Feb. 16, 1979. Copyright © American Institute of Aeronautics and Astronautics, Inc., 1979. All rights reserved. Reprints of this article may be ordered from AIAA Special Publications, 1290 Avenue of the Americas, New York, N.Y. 10019. Order by Article No. at top of page. Member price \$2.00 each, nonmember, \$3.00 each. Remittance must accompany order.

Index categories: Aerodynamics; Configuration Design; Supersonic Flow.

This paper presents a comprehensive set of conditions necessary to ensure attached flow over highly swept supersonic wings having subsonic leading edges and supersonic trailing edges. If these conditions are applied as constraints to theoretical wing design and optimization procedures, the resulting real flow will meet the low-drag, inviscid, potential-flow design goals. The paper also considers the design of other airplane components, together with the integration of these components. The design of the fuselage cannot be separate from the design of the wing, because of strong interactions at every angle of attack. Similarly, the engine installation affects the design of both the wing and the fuselage. Achievement of favorable trim drag is of great importance in the design of supersonic airplanes. This, in turn, is strongly influenced by the location of the airplane center of pressure, which depends upon the design of all airplane components and their interaction.

Results presented in this paper are based on work that began in the late 1950s and was carried through the U.S. SST program until cancellation of the program in 1971. The object of the work was to develop methods for the design of efficient supersonic airplanes. More recently, interest in the design of such airplanes has been renewed, for both eventual commercial<sup>3</sup> and military<sup>4</sup> applications. For the latter case, not only does the designer require low drag at cruising conditions, but he also requires a reasonable flow at the higher lift coefficients associated with military maneuvers. A review of design methods to accomplish this is, therefore, timely and appropriate, and forms the subject of this paper.

Theoretical methods applicable to the aerodynamic design of supersonic airplanes are reviewed in Sec. II. In Sec. III, the basic characteristics of supersonic wing planforms are discussed, and the advantages of highly swept wings in supersonic flow are pointed out. This is followed by a review of some experimental results that illustrate the basic flow problems of highly swept wings. Potential effects of warping the surface of such wings (e.g., camber and twist) are discussed in Sec. IV. The different possibilities of flow separation on highly swept, warped wings are discussed in Sec. V, with emphasis on shockwave-induced separation. Constraints for the design of highly swept supersonic wings are presented in Sec. VI. In Sec. VII, these design constraints are used to explain the development of separated flow on a number of wind-tunnel models. The use of these constraints in the design of supersonic wings is also described. General application of these methods to the airplane components is discussed in Sec. VIII.

## II. Theoretical Methods

The design approach discussed in this paper is based on the use of potential flow theory restricted to meet certain constraints. These constraints have been derived from experimental and analytical studies, and with the use of simple flow analogies, as will be discussed later. The basis of the theory is the powerful method of small disturbances that leads to the linearized potential flow equations. These equations are modified in some instances for certain nonlinear effects, with the help of higher approximations. A comprehensive presentation of the basic theory may be found in Refs. 5 and 6. Practical applications of these theories to the design and analysis of supersonic airplanes, by means of high-speed digital computers, are described in detail in Refs. 7, 8, and 9.

A procedure that has been found to be particularly useful is the supersonic design and analysis system described in detail in Ref. 7. A feature of this system is the combination of linearized aerodynamic theory with higher-order theory that accounts for shock wave formation. This system also allows the inclusion of empirical design constraints, such as presented in this paper, directly into the aerodynamic design process.

## III. Aerodynamics of Highly Swept Wings

The aerodynamic efficiency of an airplane is characterized by its lift/drag ratio,  $L/D$ . The drag of a supersonic configuration typically consists of the skin friction drag, wave drag due to thickness, and drag-due-to-lift. Supersonic drag due to lift includes both induced drag and wave drag-due-to-lift. The theoretical drag polar (that is, the relationship between drag and lift) for any simple configuration can be expressed as

$$C_D = C_{D_0} + \left( \frac{\partial C_D}{\partial C_L^2} \right) C_L^2$$

where  $C_{D_0}$  is the drag coefficient at zero lift, and is composed of both thickness wave drag  $C_{D_W}$  and friction drag  $C_{D_F}$ . The drag-due-to-lift factor  $\partial C_D / \partial C_L^2$  is theoretically independent of the lift coefficient. The solution of this equation for maximum  $L/D$  gives the simple relation

$$(L/D)_{\max} = \frac{0.5}{\sqrt{C_{D_0} \left( \frac{\partial C_D}{\partial C_L^2} \right)}}$$

Hence, the attainment of high  $(L/D)_{\max}$  is seen to depend on the two factors,  $C_{D_0}$  and  $(\partial C_D / \partial C_L^2)$ . The drag-due-to-lift factor is primarily affected by the wing selection. The friction drag is primarily determined by the Reynolds number and Mach number. The thickness wave drag is dependent on the wing planform shape and its thickness distribution.

Increased wing sweep, so that the leading edge is behind the leading-edge shock (subsonic leading edge) as shown in Fig. 1, is very beneficial in reducing both thickness wave drag and the drag-due-to-lift factor. Additional reductions in the drag-due-to-lift factor are indicated by carving out the less efficient aft area of a delta wing, thereby producing an "arrow" wing planform.

### High-Swept-Wing Experimental Results

Results of wind-tunnel tests to substantiate the low drag levels of highly swept, supersonic wings are shown in Figs. 2 and 3. The results indicate that the predicted drag levels at zero lift are indeed achieved. However, the drag-due-to-lift factor is substantially higher than theoretical predictions, particularly when the leading edge is subsonic.

The wind-tunnel results<sup>10,11</sup> shown in Fig. 3 associated the increased drag-due-to-lift with a sudden change in the upper-surface flow from an attached flow to a separated flow condition. The theoretical model and observed flow patterns are shown in Fig. 4. The observed pattern was dominated by the formation of a leading-edge separation vortex, characteristic of the flow pattern found on highly swept wings at subsonic speeds.<sup>12</sup>

### Flow Over a Highly Swept Wing

By virtue of extensive experimental and semiempirical investigations,<sup>13-19</sup> the formation of the leading-edge separation vortex is well understood. For the subsonic leading-edge wing at angle of attack, there is flow from the lower surface around the leading edge to the upper surface. The line where the streamlines split, between the flow around to the upper surface and the flow back on the lower surface, is called the "dividing streamline." The expansion of the flow going around the leading edge from the dividing streamline results in a very high negative pressure, and a subsequent steep adverse pressure recovery gradient near the leading edge on the upper surface. The steep adverse pressure recovery gradient can readily cause the three-dimensional boundary layer to separate from the surface. When separation occurs, the boundary layer leaves the wing surface along a swept

Fig. 1 Supersonic wing planforms.

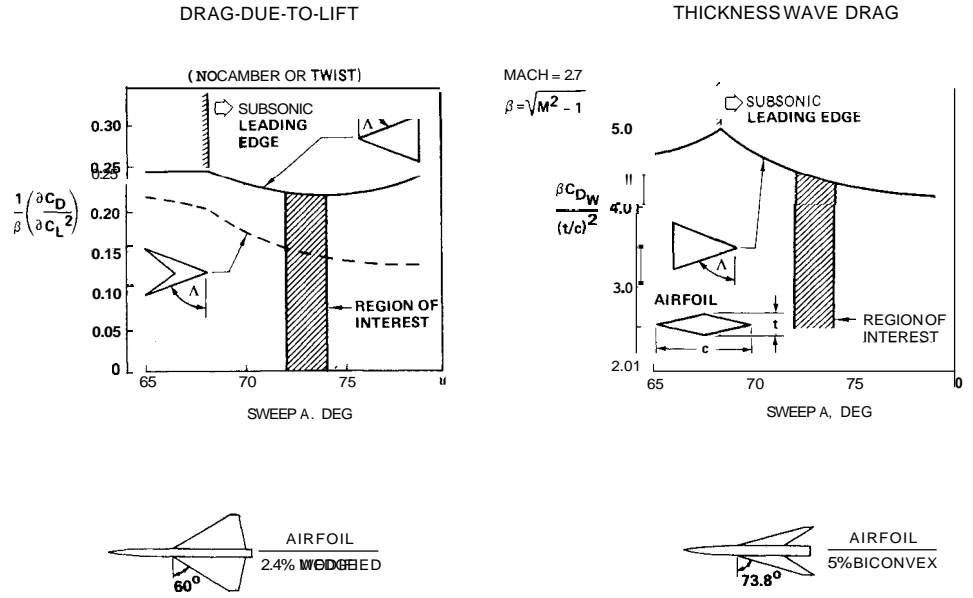


Fig. 2 Comparison of theory with experiment for symmetric supersonic wings.

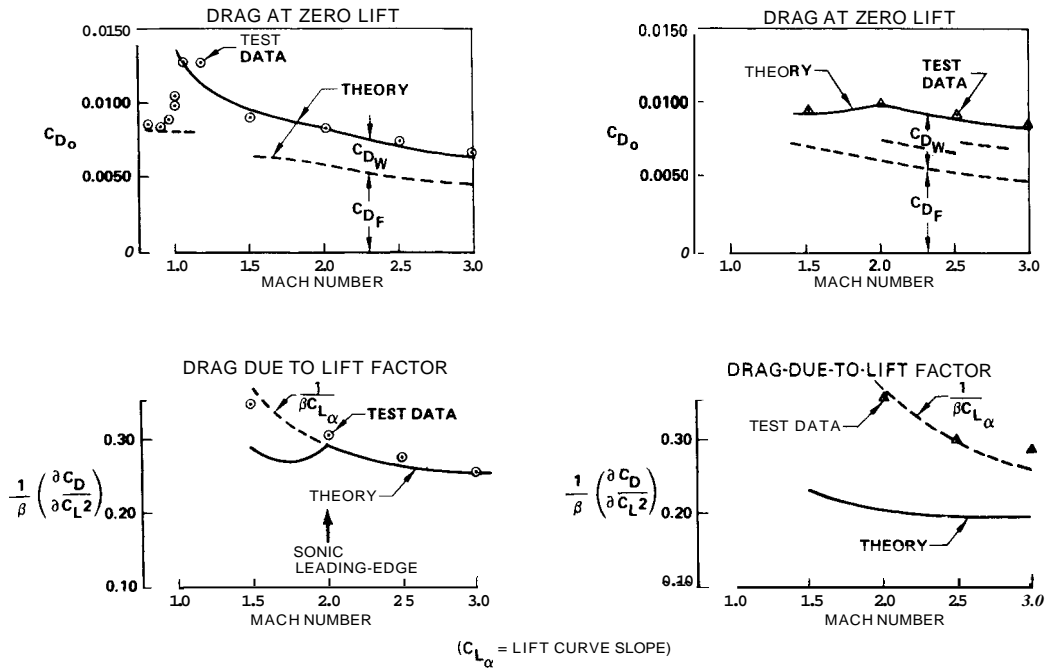
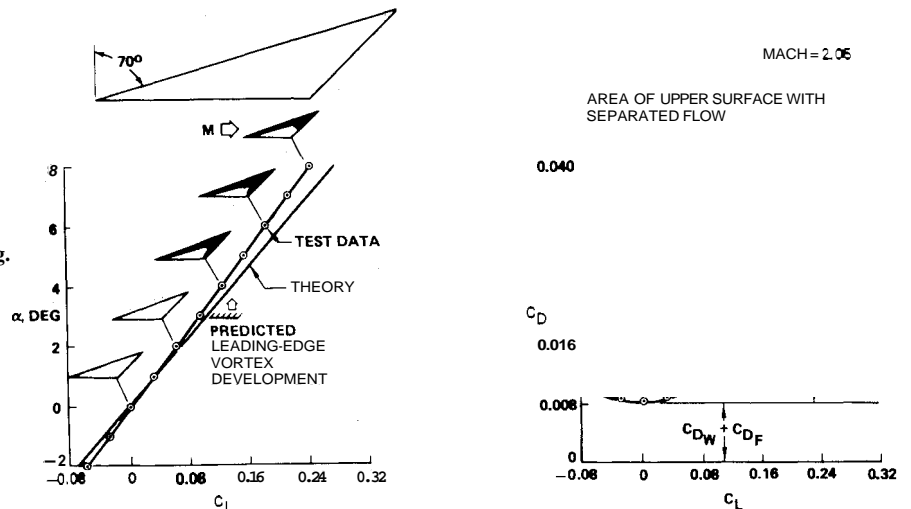


Fig. 3 Lift and drag of a highly swept flat wing.



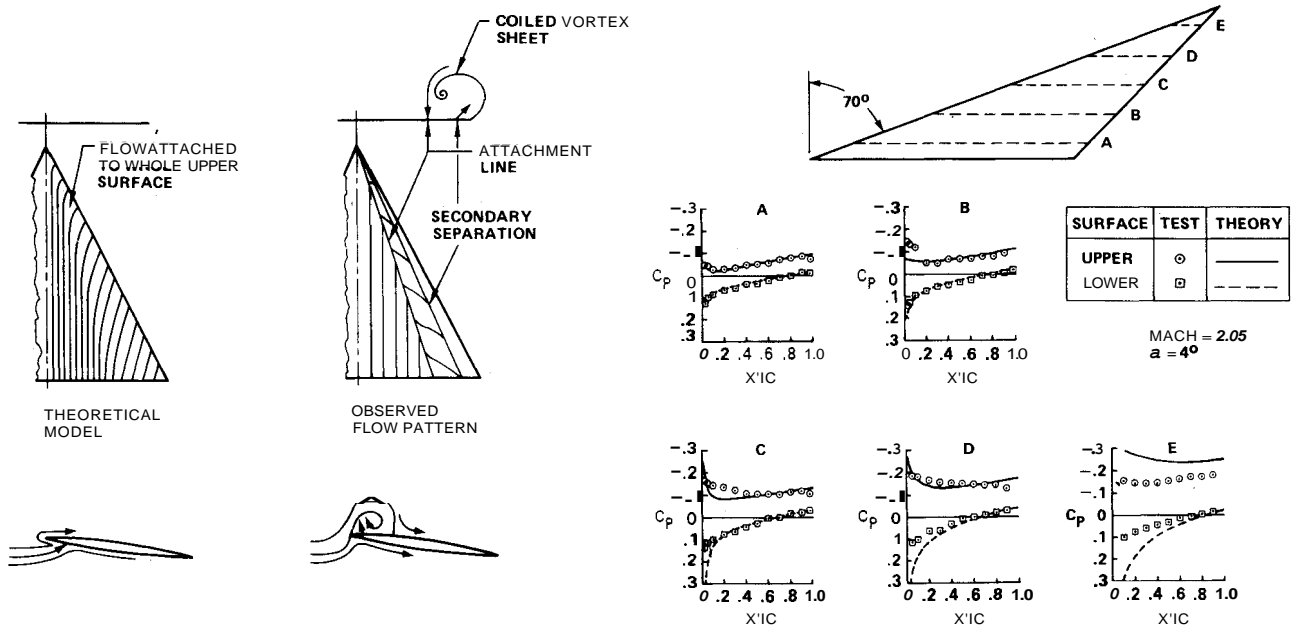


Fig. 4 The practical problem of the highly swept wing.

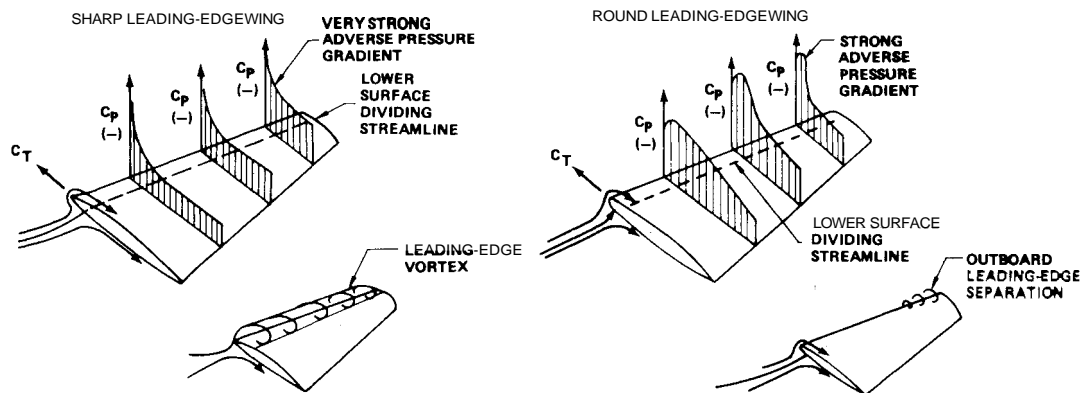


Fig. 5 Pressure distribution on highly swept flat wings.

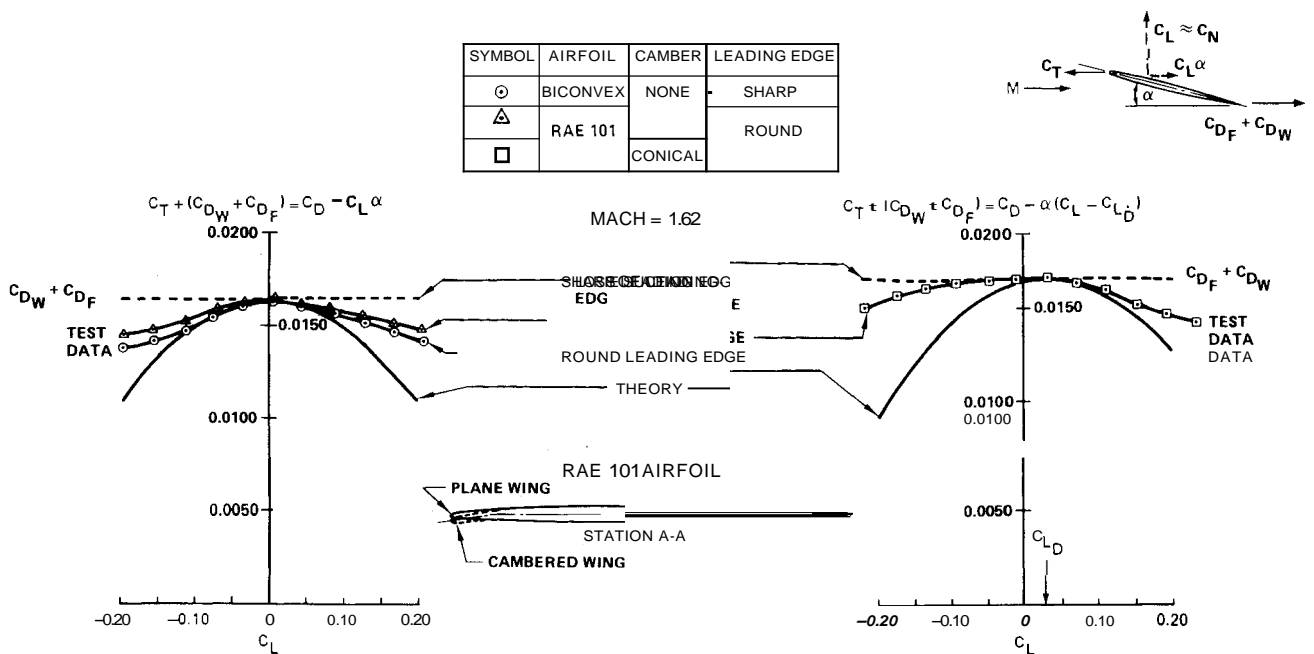


Fig. 6 Effect of airfoil geometry on chord force.

separation line and rolls up into a region of concentrated vorticity that is swept back over the upper surface of the wing. The effect of this vortex is to alter the velocity distribution and, hence, the pressure distribution over the wing. The pressure distributions<sup>19</sup> in Fig. 4 illustrate the effect of the leading-edge vortex on the upper surface. Note that the lower-surface pressures are also affected. The lower-surface effect is associated with the dividing streamline's moving to the leading edge when the leading-edge vortex is formed.

Typical pressure distributions and leading-edge vortex formation on two highly swept wings, with sharp and with round leading-edge airfoils, are shown in Fig. 5. The leading-edge vortex springs from the entire leading edge of the sharp airfoil wing. The effect of the round leading edge is to reduce the adverse pressure gradient on the inboard portion of the wing. The leading-edge separation starts near the wingtip and moves inboard with increasing angle of incidence. The formation of the leading-edge vortex affects the lift, pitching moment, and drag on a highly swept wing.<sup>18</sup>

Discussions in this paper are primarily concerned with the effect on drag. The theoretical drag force on a wing section, as shown in Fig. 6, is the resultant of a component of the surface normal force ( $C_L \alpha$ ), the thickness wave drag, friction drag, and a leading-edge thrust force  $C_x$ . In practice, the thrust force must develop from the negative leading-edge pressure acting on the "nose" of the airfoil.

Experimental variations of the leading-edge thrust force obtained on a highly swept delta wing<sup>20</sup> are compared with theoretical predictions in Fig. 6, for two symmetrical (flat) wings and for a wing with conical camber. One of the two flat wings had a sharp leading-edge airfoil. The other flat wing and the wing with conical camber had rounded leading edges. Note that the flat wing loses the theoretically predicted thrust force at very low lift coefficients ( $C_x = 0.05$ ). The rounded leading-edge airfoil is able to achieve a higher percentage of the leading-edge thrust force than the wing with a sharp airfoil. This loss in leading-edge thrust force is directly associated with the formation of the leading-edge vortex. The conically cambered wing is able to achieve the predicted thrust force to a higher lift coefficient ( $C_{LD} = 0.075$ ). However, at negative lift coefficients, little if any leading-edge suction is achieved.

**Leading-Edge Separation Criteria**

It has been found that the nature of the flow over highly swept wings at incidence changes with increasing Mach number, from a leading-edge-separation type of flow to an attached flow over the upper surface of the wing.<sup>14</sup> On thin wings, this can occur at a Mach number below that for which

the leading edge is supersonic (i.e., the component of Mach number normal to the leading edge is less than 1).

In the analyses of separated flow around swept leading-edge wings, it has been found useful to correlate the data in terms of conditions normal to the leading edge. The velocity components normal to the plane of the wing  $W_N$ , and normal to the leading edge of the wing in the plane of the wing  $U_N$  are

$$W_N = U \sin \alpha$$

$$U_N = U \cos \alpha \cos \Lambda$$

The incidence angle normal to the leading edge  $\alpha_N$  and the normal Mach number  $M_N$  are

$$\alpha_N = \tan^{-1} \left( \frac{W_N}{U_N} \right) = \tan^{-1} (\tan \alpha / \cos \Lambda)$$

$$M_N = M \cos \Lambda \sqrt{1 + \sin^2 \alpha \tan^2 \Lambda}$$

As shown in Fig. 7, the normal angle of incidence is appreciably higher than the wing angle of incidence  $\alpha$  for a highly swept wing. Experimental correlations of flow over highly swept uncambered wings<sup>14</sup> have identified the boundary region, as shown in Fig. 7, that separates the conditions (normal Mach number and normal incidence angles) for which attached flow or leading-edge-separation flow exist. This boundary between separated and attached flow for uncambered wings can be approximated by the expression<sup>21</sup>

$$M_N = 0.6 + 0.013 \alpha_N$$

A round leading edge, as shown in Fig. 7 and as previously discussed, tends to suppress the formation of separated flow to larger incidence angles, relative to sharp leading-edge airfoils. The leading-edge vortex formation boundaries shown in Fig. 8 have been constructed using the aforementioned sharp leading-edge airfoil separation equation to illustrate the effect of wing leading-edge sweep. This separation criterion does predict the sudden formation of the leading-edge separation vortex on the flat wing model that was shown in Fig. 3.

This flat wing separation criterion can also be applied to wings with varying leading-edge sweep by using the local leading-edge sweep angle,<sup>14</sup> as shown in Fig. 9.

To obtain the low drag potential of highly swept wings, leading-edge separation must be avoided. Otherwise, the leading-edge thrust previously discussed cannot be achieved.

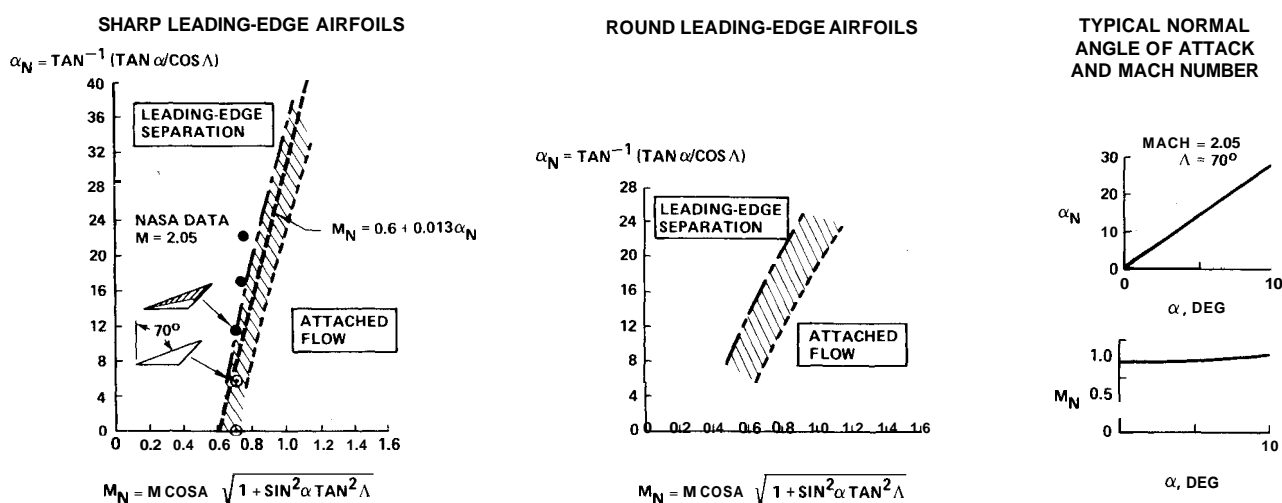


Fig. 7 Flat wing leading-edge separation boundaries.

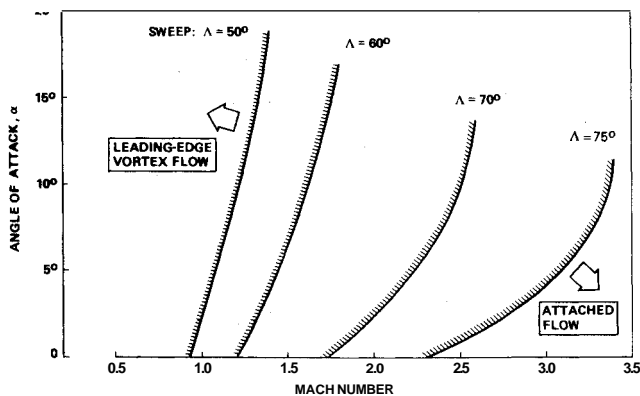


Fig. 8 Leading-edge vortex formation boundaries for flat sharp swept wings.

Hence, the low drag-due-to-lift potential of swept flat wings appears to be unachievable for all but very low incidence angles.

IV. Cambered and Twisted Wings

Properly designed warped wings can suppress the development of the leading-edge vortex and thereby shift the boundary for attached flow up to higher incidence angles (Fig. 9).

The effect of wing camber and twist (wing warp) on suppressing the leading-edge separation is shown qualitatively in Fig. 10. Wings designed to achieve a finite load distribution along the leading edge are cambered and twisted, such that the leading edges of the wing align with the local flow direction. The dividing streamline lies along the leading edge. The expansion over the wing upper surface is greatly reduced, thereby eliminating the strong adverse pressure gradient near the leading edge. The thrust force on a cambered airfoil is achieved by action of the reduced expansion pressure on the relatively large "shoulder" area of the airfoil.

At angles of attack above or below the design incidence of a warped wing, the dividing streamline will move below or above the leading edge, respectively; eventually the flow around the leading edge will result in formation of the leading-edge vortex. At negative incidence, an adverse pressure gradient rapidly develops on the lower surface and quickly eliminates the leading-edge thrust force. Data shown in Fig. 6 illustrates incidence effects on the chord force of a cambered wing.

Typical pressure distributions for warped and flat highly swept, supersonic wings are shown in Fig. 11. In addition to suppressing the formation of leading-edge separation, cambered wings offer low drag-due-to-lift potential, without the need for leading-edge thrust. This low drag-due-to-lift potential is actually slightly lower than the theoretical, but apparently unachievable, flat wing potential. A great deal of experimental and theoretical study, directed at developing low drag-due-to-lift cambered wings, has achieved widely varying results. Some of the cambered-wing designs, such as those shown in Figs. 12 and 13, achieved significant aerodynamic improvements over comparable flat wings having the same planforms and thickness distributions. The cambered wings in Fig. 12 achieved a 10% improvement in  $L/D$ . The cambered wings of Fig. 13 achieved improvement in  $L/D$  of 16% to 25% at the respective design Mach numbers. Significant improvements in  $L/D$  were achieved over a range of Mach numbers above and below the design Mach numbers. The improvements in  $L/D$  are wholly the result of reduced drag-due-to-lift. Other cambered-wing designs often failed to show any improvement over flat wings. To further complicate matters, a second cambered-wing design would often fail to achieve its low drag if airplane design parameters such as the wing thickness and/or design lift coefficient were increased, or if the body shape were altered.

An explanation of these differing results came from flow visualization studies, which showed that the successful configurations had attached flow over the wing upper surface. Unsuccessful wings exhibited vortex dominated flow, strong shocks, and large regions of separated flow on the upper

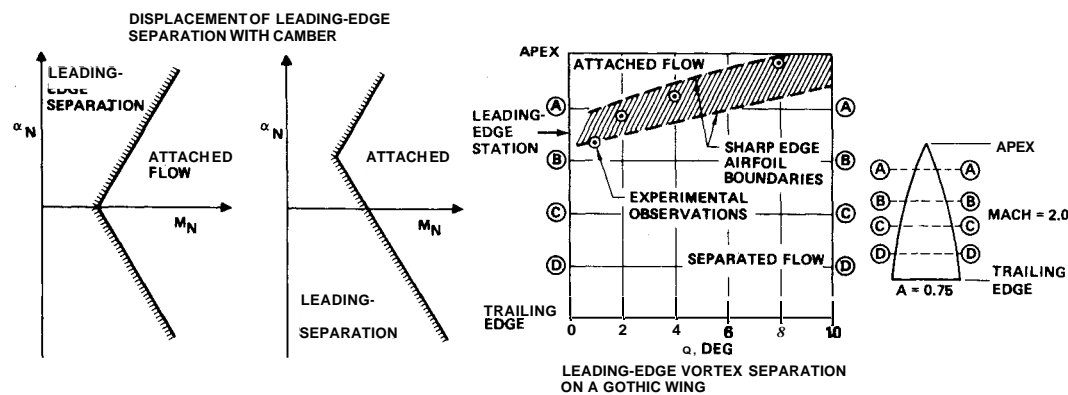


Fig. 9 Factors affecting leading-edge vortex formation boundary.

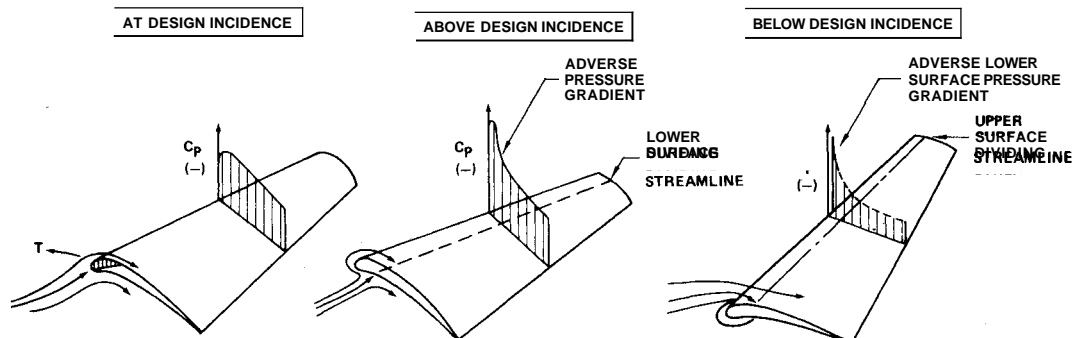


Fig. 10 Pressure distribution on highly swept cambered wings.

Fig. 11 Effect of wing camber and twist on theoretical results.

TYPICAL SUPERSONIC WING PRESSURE DISTRIBUTIONS

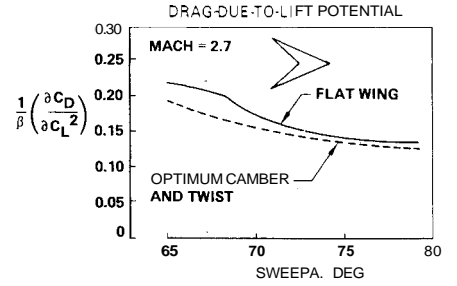
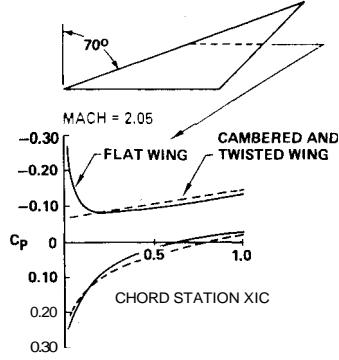


Fig. 12 Lift and drag of a highly swept cambered and twisted wing.

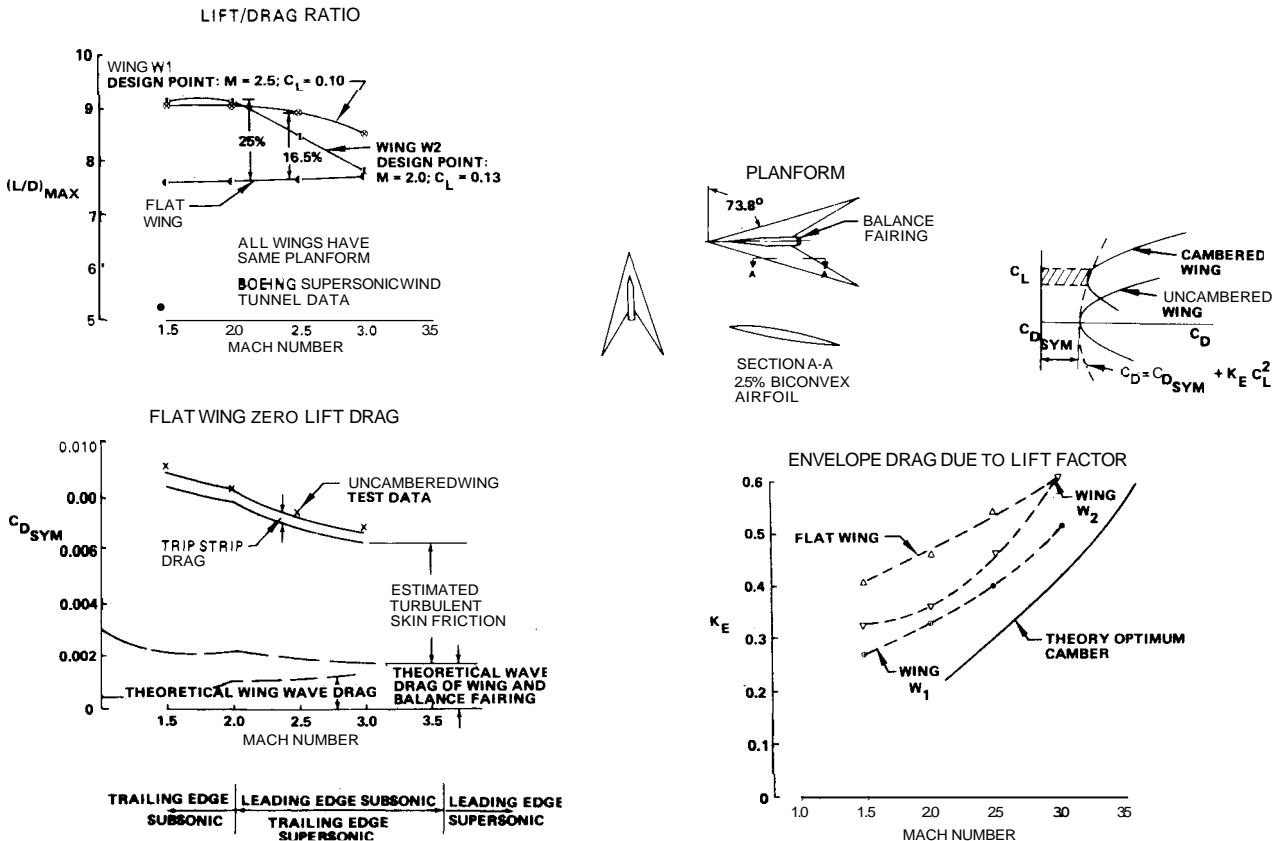
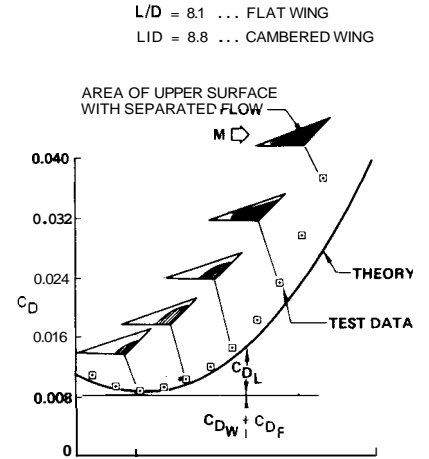
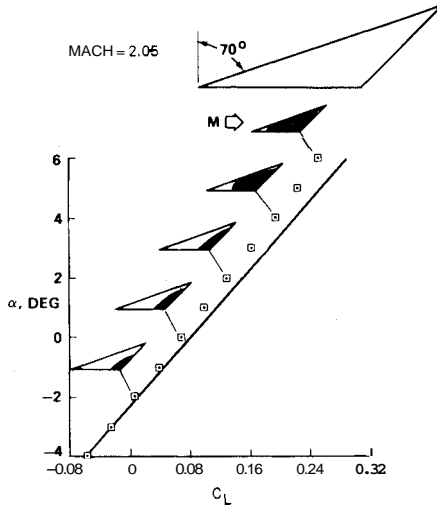


Fig. 13 The effect of camber and twist on the lift/drag ratio of highly swept wings.

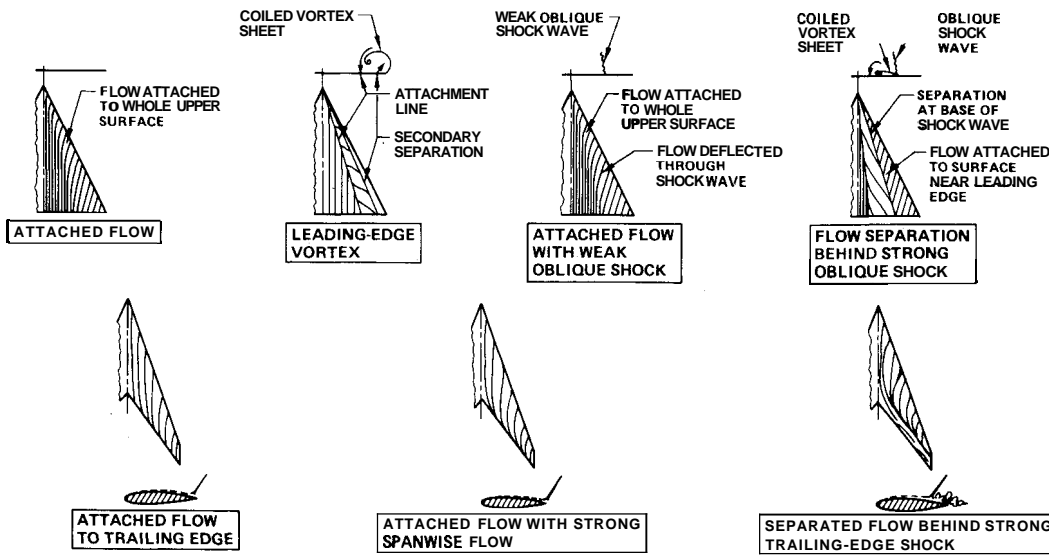


Fig. 14 Main types of flow on highly swept wings.

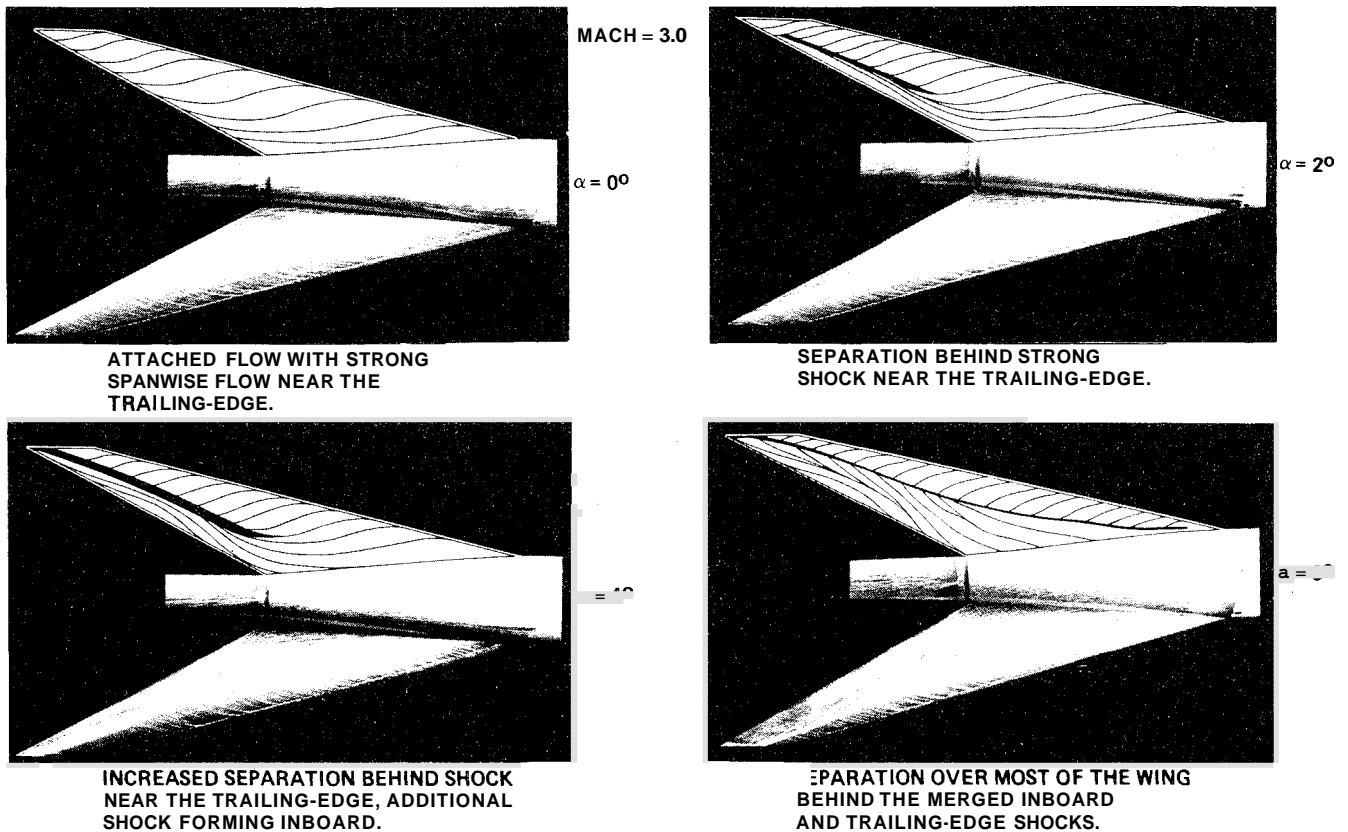


Fig. 15 Example of shock induced separation.

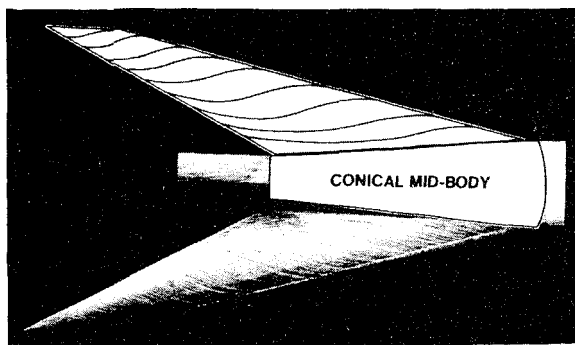
surfaces of the wings. Camber and twist design of a given configuration must take into account, therefore, the influence factors such as wing thickness, lift coefficient, design pitching moment for low trim drag, and body shape. To make this possible, a more thorough understanding of the different types of flow in these wings became necessary, as discussed below.

### V. Types of Flow on Highly Swept Wings

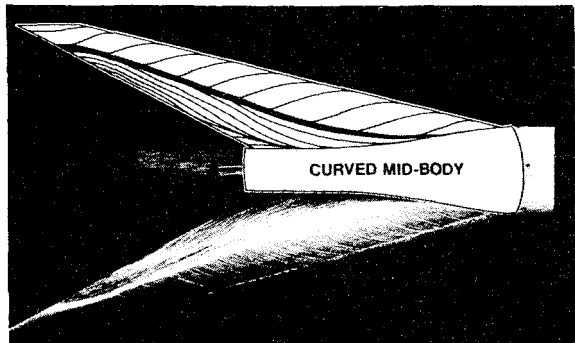
The unsuccessful cambered wings typically encountered strong spanwise flow near the trailing edge, flow separation behind a strong oblique shock near the wing leading edge, or separation behind a strong shock close to the trailing edge. The main types of flow observed on these highly swept,

cambered, supersonic wings are shown in Fig. 14. The attached flow corresponds to the theoretical conditions. The leading-edge vortex flow is characteristic of highly swept, flat wings. Often, more than one of these illustrated conditions would exist simultaneously.

Figure 15 shows a typical development of separated flow over a cambered wing at Mach 3.0 as the angle of incidence is increased. Figure 16 illustrates how a change in midbody contour can promote shock-induced flow separation. It is necessary to understand why flow separation can occur, to enable the design of configurations that will be free from this undesirable condition. An approach that can lead to the successful design of supersonic airplanes is discussed in the next section.



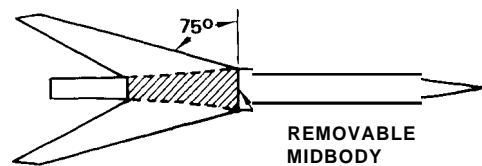
ATTACHED FLOW WITH STRONG SPANWISE FLOW NEAR THE TRAILING-EDGE



SEPARATED FLOW BEHIND STRONG BODY INDUCED SHOCK

MACH = 3.0  
 $\alpha = 0^\circ$

MODEL CONFIGURATION



BODY CROSS-SECTIONAL AREA DISTRIBUTION

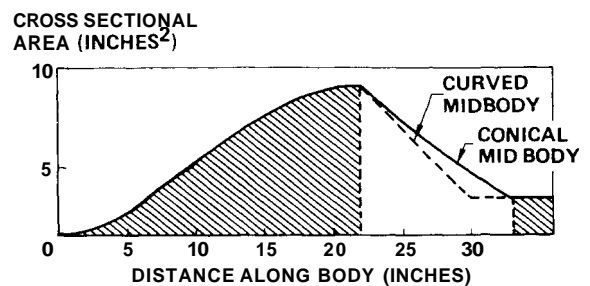
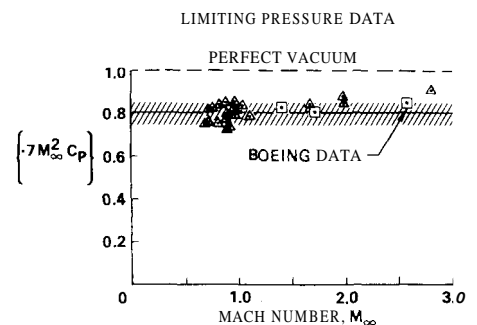
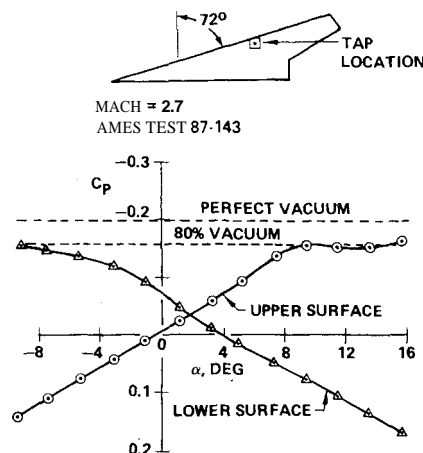


Fig. 16 Body induced shock separation.

Fig. 17 Limiting high suction pressures.



VI. Cambered-Wing Design Criteria

Careful examinations of test results have shown that the design of the wing camber and twist in conjunction with wing thickness and body effects must avoid 1) strong spanwise flow, 2) extremely high suction pressures, 3) inboard shock separation, and 4) trailing-edge shock separation.

Design criteria were needed to predict flow breakdown on the basis of potential flow analyses, so that wing camber and twist could be developed or modified to avoid serious drag increases. In general, the type of flow over a wing depends on the combination of camber, twist, angle of attack, wing thickness distribution, airfoil shape, body shape, effects of other airplane components, and flight conditions. All of these contribute to the pressure distribution on the wing. The pressure distribution directly governs the nature of the flow over the wing. The design criteria considered here were derived from a substantial body of experimental three-dimensional and two-dimensional boundary-layer separation results.

Criterion 1: Avoid High Suction Pressures

Linear theory estimates can provide theoretical negative pressures in excess of vacuum pressures. Experimental data, such as shown in Fig. 17, indicate that it is advisable to reject theoretical solutions when predicted suction pressures exceed about 70% or 80% of vacuum pressure. This can be accomplished by applying load constraints during the theoretical wing design optimization process.

Criterion 2: Avoid Strong Spanwise Flow

To avoid strong spanwise flow, it is necessary to prohibit development of increasing negative pressures near the wingtip. Theoretical studies, such as shown in Fig. 18, indicate that wing pressures due to thickness build up near the wingtip and that they form a large part of the total wingtip pressures. Fortunately, as shown in Fig. 18, the wing outboard thickness pressures are relatively insensitive to changes in the airfoil shape or thickness on the inboard wing. To limit

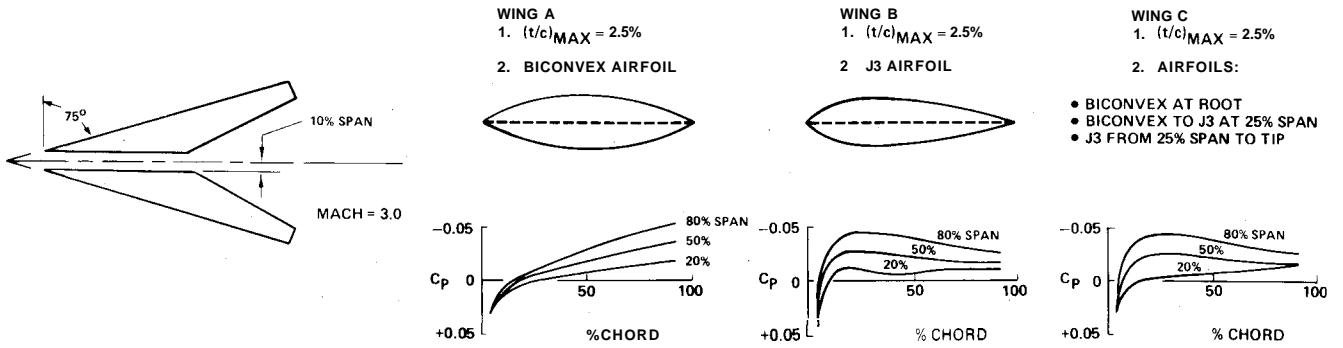


Fig. 18 Limit tip thickness to subdue strong spanwise flow.

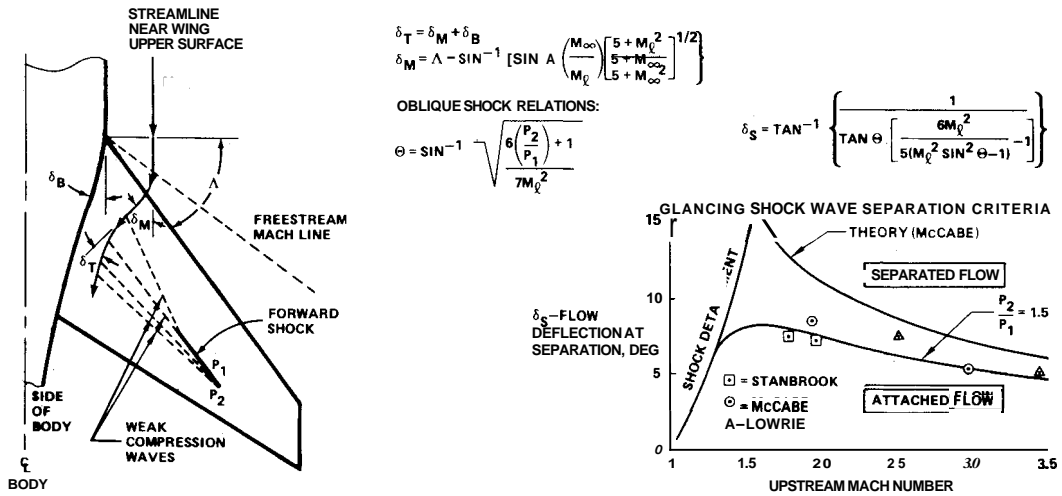


Fig. 19 Inboard shock separation criteria.

spanwise flow, the wingtip must, therefore, be kept thin. However, the inboard portion of the wing can be thickened to satisfy structural requirements without affecting the spanwise flow. It is necessary, therefore, to consider the effect of wing thickness on drag-due-to-lift optimizations, even in linearized flow calculations.

**Criterion 3: Avoid Inboard Shock Separation**

The formation of the forward shock, as shown in Fig. 19, is associated with flow conditions near the inboard portion of the wing and is therefore referred to as the inboard shock. This shock is associated with the flow near the wing leading-edge junction with the body.<sup>25,26</sup> The local flow on the upper surface of a swept wing is directed inward. The flow must then turn to run parallel to the local body surface. This subsequent turning of the flow causes compression waves; these may coalesce and form a shock wave that is swept aft at approximately the local flow Mach angle. If the required turning angle is large enough, the shock strength may become sufficiently strong to separate the boundary layer.

Empirical separation data,<sup>27-29</sup> for flow across a glancing shockwave in which the flow is deflected in the plane of the wing, indicate that a pressure rise of 50% across the shock will cause flow separation. Using single sweep theory, the local flow turning angle ( $\theta$ ) can be related to the freestream Mach number  $M_\infty$ , wing leading-edge sweep  $A$ , and local Mach number  $M_1$  (or pressure coefficient). If it is then assumed that the flow turns abruptly to parallel the body surface, the oblique shock relations can be used to calculate the pressure rise associated with this abrupt change in direction. Flow separation across a forward shock is likely to occur<sup>30</sup> when this pressure rise exceeds 50%, as shown by the experimental data in Fig. 19.

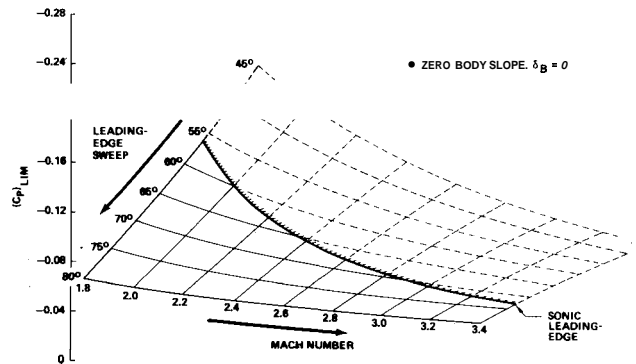


Fig. 20 Effect of sweep and Mach number on inboard shock criteria.

It is possible, therefore, to establish a limit on the allowable negative pressure coefficient level in the area of wing/body junction. This limit, which depends on the wing sweep, local body curvature, and freestream Mach number, is usually significantly more restrictive than the aforementioned 80% vacuum limit.

The equations used to calculate the inboard shock limiting of pressures are shown in Fig. 19. Figure 20 shows the effect of freestream Mach number and leading-edge sweep on the inboard limiting pressure for a straight-sided body ( $\delta_B = 0$  deg). Body contouring, as shown in Fig. 21, has a powerful effect on the allowable inboard pressures. A contracting body near the leading-edge junction typical of an area-ruled body greatly increases the allowable negative pressure, but also contributes a negative pressure field to the front portion of a wing. Hence, the net benefit of body contouring in avoiding

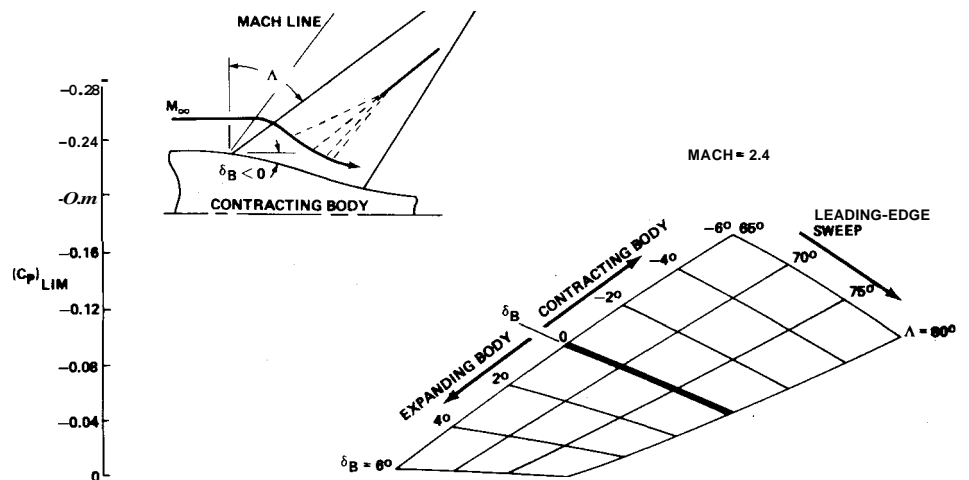


Fig. 21 Effect of body contour on inboard shock criteria.

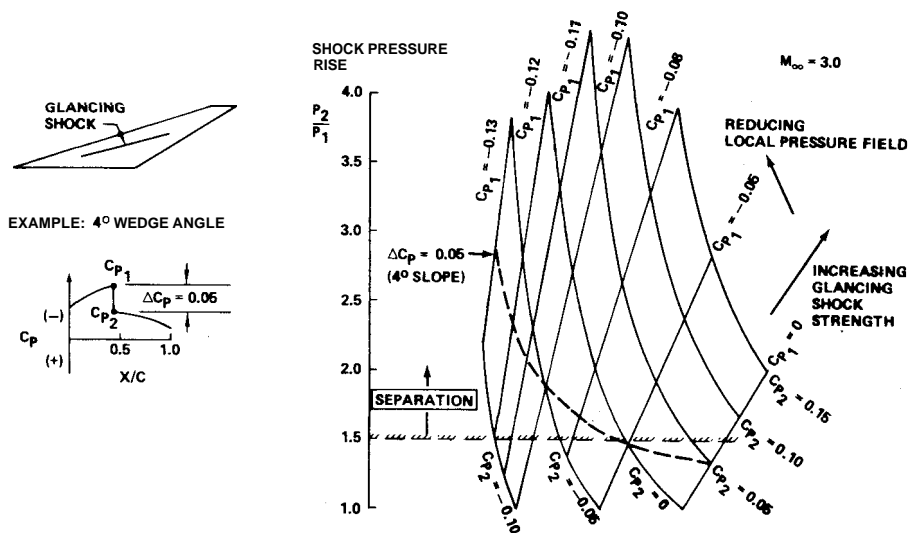


Fig. 22 Amplification of glancing shock pressure rise by local pressure field.

the formation of the inboard shock requires specific evaluation.

**Criterion 4: Avoid Shock Strength Amplification**

The same separation criterion (i.e., pressure rise of 50%) can be used to gauge the possibility of flow separation on the wing across glancing shocks produced by the body pressure fields or other adjacent components, such as nacelles, struts, or tip fins. As shown in Fig. 22, the local pressure field on the upper surface of a wing can amplify the pressure rise across a shockwave, causing a normally mild shock to promote separation. The fuselage and other nearby components can, therefore, have important effects on the design of supersonic wings.

**Criterion 5: Avoid Trailing-Edge Separation**

Wing planforms having a supersonic trailing edge develop a trailing-edge shock across which the wing upper surface pressures adjust to approximately freestream static pressure. The strength of the trailing-edge shock is directly associated with the upper surface pressure at the trailing edge. The flow across the trailing shock is quite similar to flow across a compression corner. Empirical correlations of separation data for compression corners,<sup>31,32</sup> as shown in Fig. 23, indicate that a pressure rise exceeding  $1 + 0.3M^2$  can result in flow separation. Additional experimental studies<sup>33,34</sup> of flow across swept compression corners suggest that the effect of wing trailing-edge sweep can be accounted for by the use of

the local normal Mach number ( $M_{Ni} = M_i \cos \alpha_{TE}$ ) in determining the allowable pressure rise.

Relating the Mach number normal to the trailing edge to the freestream conditions gives the limiting-edge pressures as shown in Fig. 24. Trailing-edge sweep is seen to have a powerful effect on the allowable negative pressures near the trailing edge of a highly swept wing. Except for an unswept trailing edge, this criterion is also more severely restrictive than the 80% vacuum limit.

**VII. Separation Criteria Applications**

Calculated separation criteria limiting upper surface pressures for a 75-deg swept-wing wind-tunnel model are shown in Fig. 25. The inboard shock separation-limiting pressure and the trailing edge shock separation pressure are seen to be more restrictive than the 0.8 vacuum suction pressure limit. The local body slope (-5 deg) in the area of the wing intersection nearly doubles the allowable pressure in the inboard regions of the wing. The application of these limiting pressures to this model<sup>35</sup> predicted the development of the trailing-edge shock ( $a=0$  deg, 2 deg), followed by the inboard shock ( $\alpha=4$  deg), and finally by a large area of separated flow behind the merged inboard and trailing-edge shocks ( $a=6$  deg), as shown in Fig. 15.

The design criteria have been used to explain development of the shock-induced separation on the model shown in Fig. 16 when the conical midbody section was replaced by a curved midbody.<sup>35</sup> The calculated theoretical pressures indicated that the curved midbody produced a strong midbody shock

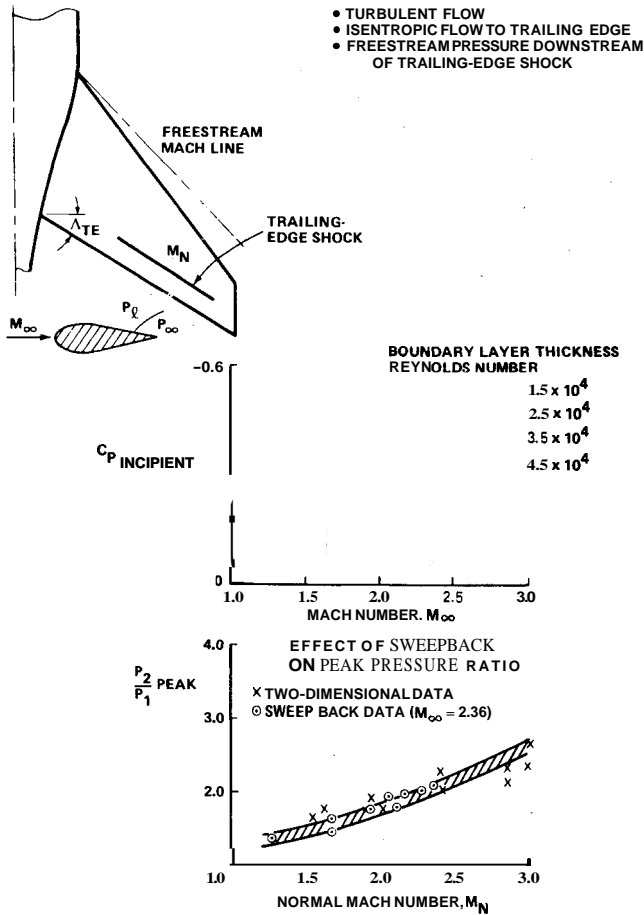


Fig. 23 Trailing-edge shock separation criteria.

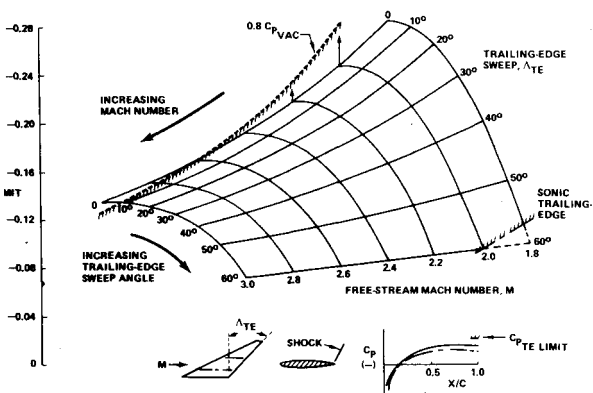


Fig. 24 Effect of trailing-edge sweep and Mach number on the trailing-edge shock separation criteria.

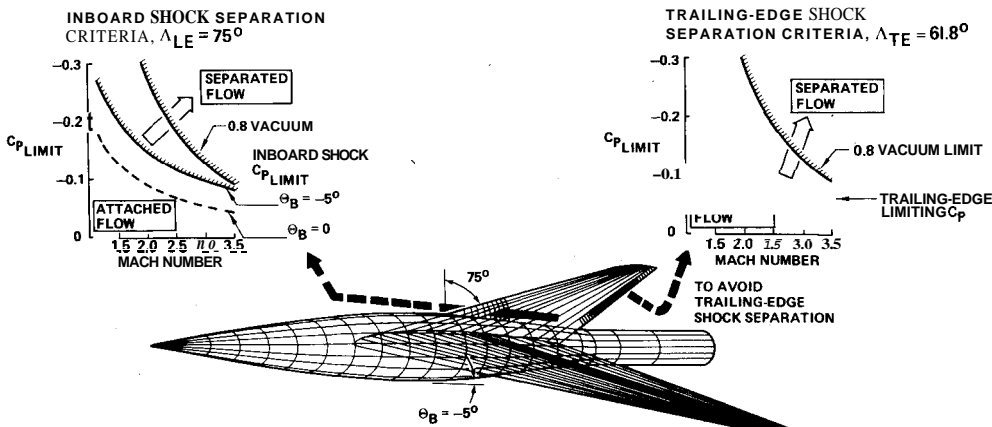


Fig. 25 Boeing wind-tunnel model flow separation criteria.

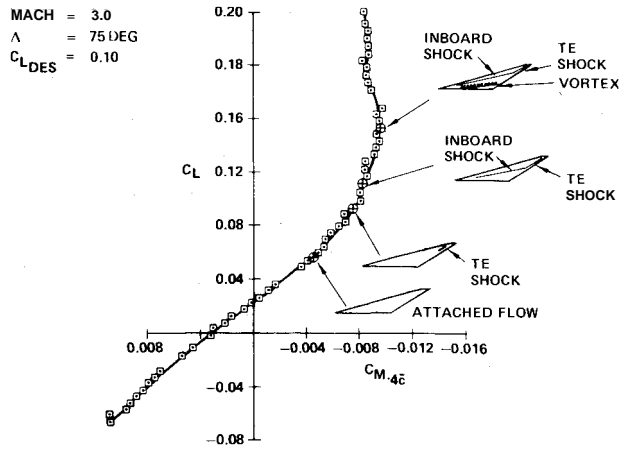


Fig. 26 Interpretation of wind-tunnel force data (Boeing wind-tunnel model).

that far exceeded the limiting pressure rise ( $P_2/P_1 = 1.5$ ) across a glancing shockwave. Figure 26 illustrates how the nonlinear pitching moment characteristics of a highly swept wing can be interpreted by means of the flow separation criteria. The initial break in the pitching moment curve is associated with loss of lift near the wingtip caused by trailing-edge separation. Severe pitchup results, as the separation behind the inboard shock rolls up into a spiral vortex sheet, shifting the wing lift inboard and forward. Additional applications of the separation criteria are shown in Ref. 35.

The recommended wing development method using the supersonic wing design criteria is summarized in Fig. 27. The wing/body combination is designed using linear theory to achieve low theoretical drag while satisfying the wing structural depth and volume requirements. The theoretical wing upper surface pressure distribution is calculated at the design condition, accounting for wing thickness, camber, twist, and body effects. The theoretical pressure distribution is checked to determine if any of the design criteria have been violated. If the design criteria are satisfied, the wing design is considered to have a high probability of success; if they are not, the design must be modified.

VIII. Applications to General Configuration Design

The previous discussions have emphasized design of the wing to achieve attached flow on the upper surface at lifting conditions. The methods are applicable, however, to other airplane components, singly or in combination.

Fuselage design, as shown in Fig. 16, should consider the adverse effects that shock waves produced by body curvature may have on the wing.

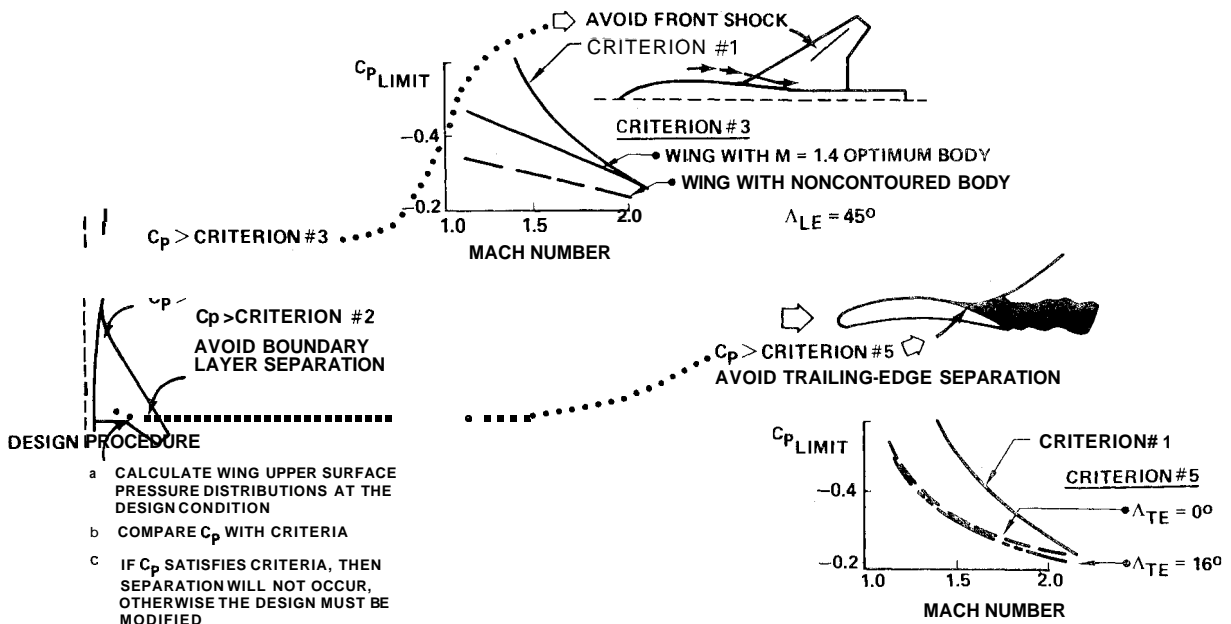


Fig. 27 Supersonic wing design criteria.

There is also a need to examine surface discontinuities associated with a cockpit. Even shocks that are initially mild can be amplified by the low-pressure field on the upper surface and ultimately lead to flow separation (Fig. 22).

The forebody angle relative to the freestream flow determines its lift and, hence, its important contribution to the center of pressure of the airplane. Care must be taken, however, to design the forebody incidence angle to prevent separation of the flow from the body, leading to a pair of counter-rotating vortices. These vortices, which provide a source of additional forebody lift and drag, may have adverse effects on the flow over the wing. The lateral stability of the airplane may also be strongly affected, particularly if the vortices impinge on the vertical tail. Real flow effects are also important in the design of the aftbody.<sup>36</sup> The design of nacelle installations for drag is discussed in Ref. 37, where it is shown that the correct installation of the propulsion system of a supersonic airplane is very configuration dependent. The engine installation must consider many factors, such as engine shape, airplane shape, and engine location. It is generally easier to install a nacelle below the wing, since the strength of the shockwave field due to the nacelle and boundary-layer diverter is actually reduced by the positive-pressure field on the wing lower surface. Conversely, great care must be taken when nacelles are installed on the upper surface of a wing. Not only is the strength of the shockwaves amplified to the degree that separation may occur, but typically, the boundary-layer diverters are deeper because of thicker boundary layers. Additionally, the nacelles are larger because of the lower pressure field on the wing upper surface at lifting conditions.<sup>38</sup>

**IX. Conclusions**

- 1) The foregoing discussions have shown that highly swept wings offer low supersonic drag levels.
- 2) Highly swept flat wings are unable to achieve the theoretically low drag-due-to-lift levels except at very small incidence angles.
- 3) Highly swept cambered and twisted wings designed for optimum load distributions with finite leading-edge pressures can achieve low drag-due-to-lift levels, providing the flow remains attached at the design condition.
- 4) Supersonic design criteria have been presented as a means of avoiding shock-induced flow separations, and thereby allowing the attached flow condition to be achieved.

The supersonic wing design methods of Ref. 7 allow the design constraints to be imposed during the wing design process.

**Acknowledgments**

Results presented in this paper are based on an effort that has covered a great many years. Several workers have made important contributions in that time period. The authors gratefully acknowledge the work of M. E. Beutow, T. H. Hallstaff, C. S. Howell, W. D. Middleton, R. C. Potter, and many others at Boeing. The authors also have made free use of whatever information was available to them from all other sources, including discussions with other workers in the field. The authors also wish to acknowledge the many helpful suggestions made by the AIAA reviewers of this paper.

**References**

- <sup>1</sup>Brown, C.E. and McLean, F.E., "The Problem of Obtaining High Lift Drag Ratios at Supersonic Speeds," *Journal of the Aeronautical Sciences*, Vol. 26, May 1959, pp. 298-302.
- <sup>2</sup>MacCormack, R.W., "Status and Future Prospects of Using Numerical Methods to Study Complex Flows at High Reynolds Numbers," AGARD-LS-94, Paper 13, Feb. 1978.
- <sup>3</sup>"*Proceedings of the SCAR Conference*," Vol. I and Vol. II, NASA CP-001, Nov. 1976.
- <sup>4</sup>"*Design Conference Proceedings: Technology for Supersonic Cruise Military Aircraft*," Vol. I and Vol. II, USAF AFFDL/FX, Feb. 1976.
- <sup>5</sup>"General Theory of High-speed Aerodynamics," *Princeton Series on High-speed Aerodynamics and Jet Propulsion*, Vol. VI, edited by W. R. Sears, Princeton University Press, Princeton, N.J., 1954.
- <sup>6</sup>"Aerodynamic Components of Aircraft at High Speeds," *Princeton Series on High-speed Aerodynamics and Jet Propulsion*, Vol. VII, edited by A. F. Donovan and H. R. Lawrence, Princeton University Press, Princeton, N.J., 1957.
- <sup>7</sup>Middleton, W.D. and Lundry, J.L., "A Computational System for Aerodynamic Design and Analysis of Supersonic Aircraft," NASA CR-2715, March 1976.
- <sup>8</sup>Carmichael, R.L. and Woodward, F.A., "An Integrated Approach to the Analysis and Design of Wings and Wing-Body Combinations in Supersonic Flow," NASA TN D-3685, Oct. 1966.
- <sup>9</sup>Woodward, F.A., Tinoco, E.N., and Larsen, J.W., "Analysis and Design of Supersonic Wing-Body Combinations, Including Flow Properties in the Near Field, Part 1—Theory and Applications," NASACR-73106, 1967.

<sup>10</sup>Carlson, H.W., "Aerodynamic Characteristics at Mach Number 2.05 of a Series of Highly Swept Arrow Wings Employing Various Degrees of Twist and Camber," NASA TMX-332, June 1960.

<sup>11</sup>Carlson, H.W., "Longitudinal Aerodynamic Characteristics at Mach Number 2.05 of a Series of Wing-Body Configurations Employing a Cambered and Twisted Arrow Wing," NASA TMX-838, May 1963.

<sup>12</sup>Ornberg, T., "A Note on the Flow Around Delta Wings," KTH-Aero TN38, Feb. 1954.

<sup>13</sup>Kuchemann, D., "Types of Flow on Swept Wings," *Journal of the Royal Aeronautical Society*, Vol. 57, Nov. 1953, pp. 683-699.

<sup>14</sup>Stanbrook, A. and Squire, L.C., "Possible Types of Flow at Swept Leading Edges," *The Aeronautical Quarterly*, Vol. 15, Feb. 1964, pp. 72-82.

<sup>15</sup>Ghorai, S.C., "Leading-Edge Vortices and Shock-Detachment Flow Over Delta Wings," *Journal of Aircraft*, Vol. 6, May-June, 1969, pp. 228-232.

<sup>16</sup>Polhamus, E.C., "A Concept on the Vortex Lift of Sharp-Edge Delta Wings Based on a Leading-Edge Suction Analogy of Vortex Lift to the Drag Due to Lift of Sharp-Edge Delta Wings," NASA TN D-4739, May 1968.

<sup>17</sup>Polhamus, E.C., "Predictions of Vortex-Lift Characteristics by a Leading-Edge Suction Analogy," *Journal of Aircraft*, Vol. 8, April 1971, pp. 193-199.

<sup>18</sup>Snyder, M.H., Jr. and Lamar, J.E., "Application of the Leading-Edge Suction Analogy to Prediction of Longitudinal Load Distribution and Pitching Moment for Sharp-Edge Delta Wings," NASA TN D-6994, Sept. 1972.

<sup>19</sup>Carlson, H.W., "Pressure Distribution at Mach Number 2.05 on a Series of Highly Swept Arrow Wings Employing Various Degrees of Twist and Camber," NASA TN D-1264, March 1962.

<sup>20</sup>Squire, L.C., Jones, J.G., and Stanbrook, A., "An Experimental Investigation of the Characteristics of Some Plane and Cambered 65° Delta Wings at Mach Numbers from 0.7 to 2.0," R.A.E., Rept. and Memo 3305, July 1961.

<sup>21</sup>Squire, L.C., "The Estimation of the Lift of Delta Wings at Supersonic Speeds," *Journal of the Royal Aeronautical Society*, Vol. 67, Aug. 1963, pp. 476-480.

<sup>22</sup>Fellows, K.A., and Carter, E.C., "Results and Analysis on Two Isolated Slender Wings and Slender Wing-Body Combinations at Supersonic Speeds, Part I, Analyses," ARC C.P. 1131, 1970.

<sup>23</sup>Manro, M.E., Bobbit, P.J., and Rogers, J.T., "Comparisons of Theoretical and Experimental Pressure Distributions on an Arrow-Wing Configuration at Subsonic, Transonic, and Supersonic Speeds," Paper No. 11, AGARD CP-204, Sept. 1976.

<sup>24</sup>Smith, A.M.O., "High-Lift Aerodynamics," *Journal of Aircraft*, Vol. 12, June 1975, pp. 501-530.

<sup>25</sup>Sigalla, A., "Design Criterion on Upper Surface Inboard Pressure Coefficient for Arrow Wings," Boeing Document D6-4142TN, Oct. 1962.

<sup>26</sup>Rogers, E.W.E. and Hall, I.M., "An Introduction to the Flow About Plane Swept-Back Wings at Transonic Speeds," *Journal of the Aeronautical Society*, Vol. 64, Aug. 1960, pp. 449-464.

<sup>27</sup>Stanbrook, A., "An Experimental Study of the Glancing Interaction Between a Shock Wave and a Turbulent Boundary Layer," ARC CP No. 555, 1960.

<sup>28</sup>McCabe, A., "The Three Dimensional Interaction of a Shock Wave with a Turbulent Boundary Layer," *The Aeronautical Quarterly*, Vol. 17, Aug. 1966, pp. 231-252.

<sup>29</sup>Lowrie, B.W., "Cross-Flows Produced by the Interaction of a Swept Shock Wave with a Turbulent Boundary Layer," Ph.D. Thesis, University of Cambridge, Dec. 1965.

<sup>30</sup>Korkegi, R.H., "A Single Correlation for Incipient Turbulent Boundary-Layer Separation Due to a Skewed Shock Wave," *AIAA Journal*, Vol. 11, Nov. 1973, pp. 1578-1579.

<sup>31</sup>Korkegi, R.H., "Comparison of Shock-Induced Two- and Three-Dimensional Incipient Turbulent Separation," *AZAA Journal*, Vol. 13, April 1975, pp. 534-535.

<sup>32</sup>Kuehn, D.M., "Experimental Investigation of the Pressure Rise Required for the Incipient Separation of Turbulent Boundary Layers in Two-Dimensional Supersonic Flow," NASA Memo 1-21-59A, Feb. 1959.

<sup>33</sup>Stalker, R.J., "Sweepback Effects in Turbulent Boundary-Layer Shock-Wave Interaction," *Journal of the Aeronautical Sciences*, Vol. 27, May 1960, pp. 348-356.

<sup>34</sup>Green, J.E., "Interactions Between Shock Waves and Turbulent Boundary Layers," R.A.E. Tech. Rept. 69069, May 1969.

<sup>35</sup>Green, J.E., "Interactions Between Shock Waves and Turbulent Boundary Layers," R.A.E. Tech. Rept. 69069, May 1969.

<sup>36</sup>Kulfan, R.M. and Sigalla, A., "Real Flow Limitations in Supersonic Airplane Design," AIAA Paper 78-147, Huntsville, Ala., Jan. 1978.

<sup>37</sup>Peake, D.J., Rainbird, W.J., and Atraghji, E.G., "Three-Dimensional Flow Separations on Aircraft and Missiles," *AZAA Journal*, Vol. 10, May 1972, pp. 567-580.

<sup>38</sup>Sigalla, A. and Hallstaff, T.H., "Aerodynamics of Powerplant Installations on Supersonic Aircraft," *Journal of Aircraft*, Vol. 5, July-Aug. 1967, pp. 273-277.

<sup>39</sup>Van Duine, A.A., Rhodes, W.W., and Swan, W.C., "Configuration Aspects of Propulsion Installation on Supersonic Transports," *AGARD Conference Proceedings*, No. 71, 1970.

## Make Nominations for an AIAA Award

THE following awards will be presented during the AIAA 13th Fluid and Plasmadynamics Conference and the AIAA 15th Thermophysics Conference, respectively, July 14-16, 1980, Snowmass, Colo. If you wish to submit a nomination, please contact Roberta Shapiro, Director, Honors and Awards, AIAA, 1290 Avenue of Americas, N.Y., N.Y. 10019 (212)581-4300. The deadline date for submission of nominations is December 3.

### Fluid and Plasmadynamics Award

"For outstanding contribution to the understanding of the behavior of liquids and gases in motion and of the physical properties and dynamical behavior of matter in the plasma state as related to needs in aeronautics and astronautics."

### Thermophysics Award

"For an outstanding recent technical or scientific contribution by an individual in thermophysics, specifically as related to the study and application of the properties and mechanisms involved in thermal energy transfer within and between solids, and between an object and its environment, particularly by radiation, and the study of environmental effects on such properties and mechanisms."